Angewandte Chemie International Edition

Electron Transfer

DOI: 10.1002/anie.200906924

Tuning the Electronic Communication between Redox Centers Bound to Insulating Surfaces**

Dodzi Zigah, Cyril Herrier, Luc Scheres, Marcel Giesbers, Bruno Fabre, Philippe Hapiot, and Han Zuilhof**

Electrons can be passed in various manners at an electrode in solution through an organic monolayer deposited on conducting surfaces such as metals, doped semiconductors, and carbonaceous materials. Three different pathways are generally considered: 1) electron tunneling through the organic layer or space;[1] 2) direct electron transfer between the surface and the redox-mediating molecule after diffusion through the pinholes/defects of the monolayer;[2–4] and 3) (when the bound monolayer is electroactive) charge exchange between bound redox centers. This complexity typically hampers an accurate estimation of the individual contributions of each pathway. Herein, we propose a general approach to solve this issue, by using well-defined mixed monolayers on silicon in combination with scanning electrochemical microscopy (SECM).

SECM has been shown to be a powerful tool to analyze redox-active monolayer or polymer-modified surfaces.[5] The major difference from many other electrochemical methods is that, in SECM, the surface is locally probed from the solution side with an ultramicroelectrode (UME) and a dissolved redox mediator. Such a configuration thus permits the characterization of electroactive layers on insulating surfaces. Therefore, the contribution of the substrate in the charge transport mechanism can be eliminated, and subsequently allows accurate determination of the bimolecular electron-transfer kinetics between attached and dissolved redox species.[6]

Recently, we used SECM in feedback mode to delineate the highly efficient electron communication between oxidizable ferrocene (Fc) centers end-capping an organic monolayer linked to an insulating n-type silicon surface.[7] Experiments were performed in the dark to minimize electrochemical oxidation.[8] The 2D charge propagation between adjacent Fc groups was so fast that the time resolution of the SECM setup only allowed a lower limit for this rate, similar to ultrafast "charge hopping" in redox polymers[3] and redox dendrimers.[9,10] To determine this rate constant accurately, this Communication combines the high monolayer quality of tailor-made mixed monolayers—to control the rate of electron communication within the redox-active monolayer—with complete electrochemical characterization of the attached redox molecule (formal potential, surface coverage). The latter can be performed by classical electrochemistry by switching the oxide-free Si substrate from insulating (dark) to conducting (illuminated). This method gives a unique way to obtain a full control over the 2D charge propagation rate between redox centers by changing the chemical environment surrounding the Fc headgroups and/or specific interactions between the organic chains.

To this aim, a Fc-terminated monolayer was diluted with electroinactive dodecenyl chains (Scheme 1). Electron transfer at these Fc-modified surfaces was probed by SECM in feedback mode in the dark and under unbiased conditions. This approach enables not only control over the surface coverage of Fc units but also protrudes the redox centers above the plane of electroinactive methyl groups.

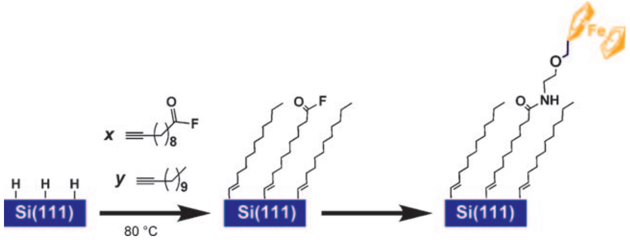

Scheme 1. Preparation of the ferrocene-terminated monolayers on n-type Si(111) surfaces.

The covalent derivatization of n-type Si(111) by the single-component Fc-terminated monolayer or mixed *n*-dodecenyl/Fc-terminated monolayer is shown in Scheme 1. In the first step, the thermal reaction of a hydrogen-terminated silicon surface (H-Si(111)) with neat 10-undecynoyl fluoride or mixtures of 10-undecynoyl fluoride and 1-dodecyne (molar ratios of 50:50 and 10:90) results in a single-component or mixed acid fluoride/methyl-terminated monolayers.[11] The ratio of acid fluoride and dodecenyl chains on the Si(111) surface was found by X-ray photoelectron spectroscopy (XPS) to be almost the same as their molar ratio in the reaction mixture (see the Supporting Information). The acid fluoride functionality proved to be both highly

---

[*] D. Zigah, C. Herrier, Dr. B. Fabre, Dr. P. Hapiot
Sciences Chimiques de Rennes
UMR 6226 CNRS/Université de Rennes 1
Matière Condensée et Systèmes Electroactifs (MaCSE)
Campus de Beaulieu, 35042 Rennes Cedex (France)
E-mail: fabre@univ-rennes1.fr

L. Scheres, Dr. M. Giesbers, Prof. Dr. H. Zuilhof
Laboratory of Organic Chemistry, Wageningen University
Dreijenplein 8, 6703 HB Wageningen (The Netherlands)
E-mail: han.zuilhof@wur.nl

[**] This work was supported by the CNRS and NanoNed, funded by the Dutch Ministry of Economic Affairs (project WSC.6972). D.Z. and C.H. thank Région Bretagne for PhD grants.

Supporting information for this article is available on the WWW under http://dx.doi.org/10.1002/anie.200906924.

reactive and selective towards amines,[11] facilitating the introduction of the Fc units with 2-aminoethylferrocenylmethylether, as previously described.[12]

Before analyzing the electron transfer kinetics by SECM, it is a prerequisite to control both the quality, the compactness, and the cleanliness of the grafted redox monolayers because such characteristics could considerably affect the electronic processes occurring at the organic layer. First, the mean thickness determined by ellipsometry of the Fc-terminated monolayers increases gradually from 15 to 19 Å as the molar fraction of 10-undecynoyl fluoride in the initial alkyne mixture is increased (Table 1). Additionally, static water contact angles decrease gradually from 105° to 69°, in line with reported values for densely packed dodecenyl (ca. 110°)[13] and other purely ferrocenyl monolayers (ca. 70°).[12,14] XPS analysis reveals characteristic peaks[15] from the Si substrate itself and from the C_{1s}, $Fe_{2p3/2}$, N_{1s}, and O_{1s} core levels of the attached molecules (Figure 1 A and the Supporting Information). The atomic force microscopy (AFM) images of electroactive monolayers show atomically flat, defect-free terraces of Si(111) with 3 Å step heights and a root mean square (rms) roughness of approximately 3.3 Å, which is not dependent on the composition of the mixed monolayers. This topography is identical to that of H-Si(111) and other ω-functionalized organic monolayers.[12,15–17]

Table 1: Principal characteristics of the ferrocene-terminated monolayers on n-type Si(111) surfaces.

Surface	Mean thickness [Å]	Contact angle [°][a]	$E^{\circ\prime}$ [V vs. SCE][b]	Ferrocene coverage [mol cm^{-2}][c]	E_{fb} [V vs. SCE][d]
Fc10	15	105	0.11	2.5×10^{-11}	−0.95
Fc50	17.5	79	0.14	2.7×10^{-10}	−1.03
Fc100	19	69	0.13	5.0×10^{-10}	−0.94

[a] With water. [b] Formal potential of the ferrocene/ferrocenium couple observed under illumination (average of anodic and cathodic peak potentials). [c] The experimental error is 1.5×10^{-11} mol cm^{-2}. [d] Flat-band potential.

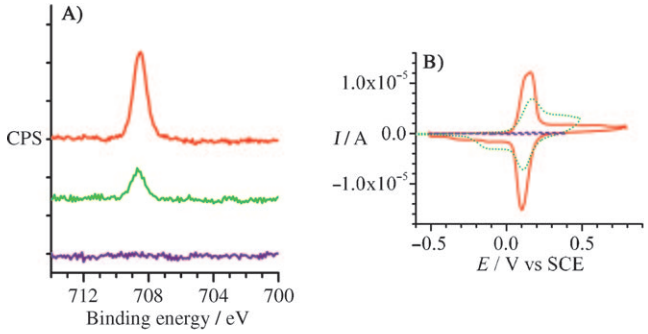

Figure 1. A) XPS $Fe_{2p3/2}$ spectra of **Fc100** (red), **Fc50** (green), and **Fc10** (purple) surfaces. CPS = Counts per second. B) Cyclic voltammograms under illumination at 0.4 V s^{-1} of **Fc100** (solid line), **Fc50** (dotted line), and **Fc10** (dashed line). Electrolyte: CH_3CN + 0.1 M Bu_4NClO_4.

Voltammetric analysis of the Fc-modified surfaces in the dark shows the absence of a significant oxidation current response. Further addition of Fc in the electrolyte solution did not modify the signal as expected for a nonconducting electrode. Upon illumination, a well-defined reversible wave assigned to the Fc/ferrocenium couple appears at $E^{\circ\prime} \approx 0.13 \pm 0.02$ V vs. SCE for the three surfaces (Figure 1 B). We note, in line with other reports,[18] that the redox potential of Fc bound to n-type Si under various illumination intensities is around 300 mV lower than that observed for Fc bound to p-type Si,[12] as a result of activation of the redox process by photogenerated electron–hole pairs.

The total surface density of attached Fc moieties (Γ_{Fc}) was estimated by integration of the cyclic voltammetry peak to be 5.0×10^{-10}, 2.7×10^{-10}, and 2.5×10^{-11} mol cm^{-2} for the surfaces prepared from neat (**Fc100**), 50 % (**Fc50**), and 10 % (**Fc10**) 10-undecynoyl fluoride, respectively (Table 1). These values correspond to surface coverages of 0.39, 0.21, and 0.02 Fc per surface silicon atom, respectively, considering that the surface density of Si(111) is 7.8×10^{14} atoms cm^{-2}.[19] A specific area of approximately 35 Å^2 per bound Fc moiety was deduced for the single-component surface, which is in line with the ball-like shape of the Fc molecules with a diameter of 6.6 Å, and indicative for a densely packed Fc monolayer.

SECM approach curves were recorded using three Fc-based redox mediators that display increasing values of the formal potential. Two of the mediators (dimethylferrocene ($FcMe_2$) and dissolved Fc) display a more positive formal potential $E^{\circ\prime}$ (0.32 and 0.40 V vs. SCE, respectively) than that of grafted Fc, and consequently could be used to oxidize the bound Fc (Fc_{surf}) centers. The third one (decamethylferrocene, $FcMe_{10}$) has a less positive $E^{\circ\prime}$ (0.0 V vs. SCE) and consequently could not oxidize Fc_{surf}. It should be noted that the $E^{\circ\prime}$ values of the three mediators are much more positive than the flat-band potential E_{fb}[20] of modified Si surfaces (ca. −1.0 V vs. SCE, Table 1 and the Supporting Information), and, thus, the regeneration of their reduced form at the n-Si(111) surface is expected not to occur in the dark. Therefore, the regeneration of the dissolved mediator involves only the bimolecular electron transfer reaction with Fc_{surf}. In the case of $FcMe_{10}$, for all electroactive monolayers, the normalized current (I_t) at a platinum UME tip approaching the modified surface rapidly diminishes as the distance d between the UME and the substrate decreases (Figure 2). The curves fit the theoretical curve expected for an insulating surface. This result reflects the absence of regeneration of the mediator at the interface (negative feedback), as expected on the basis of the difference of redox potentials.

However, when the mediator is Fc or $FcMe_2$, regeneration of the reduced form of the mediator by Fc_{surf} is now possible with a rate depending on both the nature of the mediator and the value of Γ_{Fc}. The experimental approach curves were fitted with the Bard–Mirkin formalism[5] to extract the apparent rate constants k_{app} (apparent charge transfer kinetics between the oxidized mediator and the layer). Interestingly, a linear dependence of k_{app} with Γ_{Fc} is observed for Fc and $FcMe_2$ (Figure 2 D), which reflects the variations in the electron-transfer kinetics at the layer, switching from an extremely slow to very fast process. Under our conditions, the

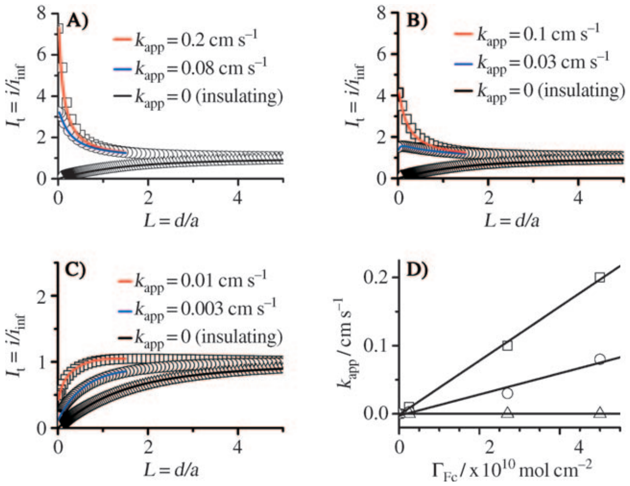

Figure 2. SECM approach curves in the dark obtained at a Pt disk UME tip (radius: 5 μm) on the **Fc100** (A), **Fc50** (B), and **Fc10** (C) modified n-type Si(111) surfaces, using Fc (□), FcMe$_2$ (○) and FcMe$_{10}$ (△) as redox mediators (1 mM in DMF + 0.1 M Bu$_4$NClO$_4$). D) Plots of k_{app} vs. Γ_{Fc} for the three redox mediators Fc (□), FcMe$_2$ (○), and FcMe$_{10}$ (△).

overall SECM process includes the following steps: 1) mass transfer in the tip/substrate gap; 2) bimolecular electron transfer between the dissolved mediator and Fc$_{surf}$; 3) electron hopping between adjacent Fc$_{surf}$; and 4) the ejection of positive charges that occurs on large areas outside the diffusion cone of the UME (to balance the injection of positive charges near the electrode).[6] Slopes of 4.0×10^8 and 1.6×10^8 mol^{-1}cm^{3}s^{-1} could be derived for Fc and FcMe$_2$, respectively, from the linear k_{app} versus Γ_{Fc} plots. In view of the relative magnitude of the rate constants corresponding to the steps 2 and 3 (see the Supporting Information), and also considering step 4 as a fast and efficient process,[7] the rate-limiting step of the overall mechanism can confidently be assigned to electron hopping. This result indicates that the observed k_{app} variations are directly correlated to the kinetics of lateral charge propagation that depends on the mean distance between two adjacent Fc centers and thus Γ_{Fc}.[3]

In conclusion, we have demonstrated in this study that the electronic communication to Fc centers bound to an insulator can be simply and efficiently controlled by the surface coverage of the electroactive units and the nature of the dissolved mediator. A straightforward linear relationship between k_{app} and Γ_{Fc} was observed. This observation opens up a promising platform for the design of novel electrochemical sensors and other electrochemically switchable systems based on insulating substrates, such as redox-based Boolean logic gates.[21]

Experimental Section

Electroactive monolayer preparation: We followed a previously reported procedure for preparation of the acid fluoride functionalized monolayers.[11] The hydrogen-terminated n-type Si(111) surfaces were immersed in argon-saturated neat 10-undecynoyl fluoride or mixtures with 1-dodecyne (GC purity of both compounds >99.9%) at 80°C and approximately 10 mbar. The reaction was stopped after 16 h and the monolayers were rinsed extensively with CH$_2$Cl$_2$ and sonicated for 5 min in CH$_2$Cl$_2$ to remove physisorbed molecules.

The single-component and mixed acid fluoride terminated monolayers were then immersed in a 25 mM solution of 2-aminoethylferrocenyl methyl ether in CH$_2$Cl$_2$ for 30 min. Afterwards, samples were rinsed and ultrasonicated with CH$_2$Cl$_2$.

Received: December 8, 2009
Revised: February 1, 2010

Keywords: electron transfer · ferrocene · monolayers · silicon · surface chemistry

[1] a) J. F. Smalley, S. W. Feldberg, C. E. D. Chidsey, M. R. Linford, M. D. Newton, Y. P. Liu, *J. Phys. Chem.* **1995**, *99*, 13141–13149; b) O. Yaffe, L. Scheres, S. R. Puniredd, N. Stein, A. Biller, R. H. Lavan, H. Shpaisman, H. Zuilhof, H. Haick, D. Cahen, A. Vilan, *Nano Lett.* **2009**, *9*, 2390–2394.

[2] B. Ulgut, H. D. Abruña, *Chem. Rev.* **2008**, *108*, 2721–2736, and refs. therein.

[3] J.-M. Savéant in *Elements of Molecular and Biomolecular Electrochemistry*, Wiley-VCH, Weinheim, **2006**.

[4] H. O. Finklea in *Encyclopedia of Electrochemistry*, *Vol. 10* (Eds.: A. J. Bard, M. Stratmann, I. Rubinstein, M. Fujihira, J. F. Rusling), Wiley-VCH, Weinheim, **2007**, pp. 623–650.

[5] a) A. J. Bard, M. V. Mirkin in *Scanning Electrochemical Microscopy*, Marcel Dekker, New York, **2001**; b) G. Wittstock, M. Burchardt, S. E. Pust, Y. Chen, C. Zhao, *Angew. Chem.* **2007**, *119*, 1604–1640; *Angew. Chem. Int. Ed.* **2007**, *46*, 1584–1617; c) S. Amemiya, A. J. Bard, F. R. F. Fan, M. V. Mirkin, P. R. Unwin, *Annu. Rev. Anal. Chem.* **2008**, *1*, 95–131; d) C. Wei, A. J. Bard, M. V. Mirkin, *J. Phys. Chem.* **1995**, *99*, 16033–16042; e) A. L. Whitworth, D. Mandler, P. R. Unwin, *Phys. Chem. Chem. Phys.* **2005**, *7*, 356–365; f) L. H. Lie, M. V. Mirkin, S. Hakkarainen, A. Houlton, B. R. Horrocks, *J. Electroanal. Chem.* **2007**, *603*, 67–80.

[6] B. Liu, A. J. Bard, M. V. Mirkin, S. E. Creager, *J. Am. Chem. Soc.* **2004**, *126*, 1485–1492.

[7] F. Hauquier, J. Ghilane, B. Fabre, P. Hapiot, *J. Am. Chem. Soc.* **2008**, *130*, 2748–2749.

[8] X. G. Zhang in *Electrochemistry of Silicon and its Oxide*, Kluwer/Plenum, New York, **2001**.

[9] C. Amatore, Y. Bourret, E. Maisonhaute, J. I. Goldsmith, H. D. Abruña, *ChemPhysChem* **2001**, *2*, 130–134.

[10] a) C. Ornelas, J. R. Aranzaes, E. Cloutet, S. Alves, D. Astruc, *Angew. Chem.* **2007**, *119*, 890–895; *Angew. Chem. Int. Ed.* **2007**, *46*, 872–877; b) A. Wang, C. Ornelas, D. Astruc, P. Hapiot, *J. Am. Chem. Soc.* **2009**, *131*, 6652–6653; c) C. A. Nijhuis, J. K. Sinha, G. Wittstock, J. Huskens, B. J. Ravoo, D. N. Reinhoudt, *Langmuir* **2006**, *22*, 9770–9775.

[11] L. Scheres, J. ter Maat, M. Giesbers, H. Zuilhof, *Small* **2010**, *6*, 642–650.

[12] B. Fabre, F. Hauquier, *J. Phys. Chem. B* **2006**, *110*, 6848–6855.

[13] a) L. Scheres, A. Arafat, H. Zuilhof, *Langmuir* **2007**, *23*, 8343–8346; b) Q.-Y. Sun, L. C. P. M. de Smet, B. van Lagen, M. Giesbers, P. C. Thüne, J. van Engelenburg, F. A. de Wolf, H. Zuilhof, E. J. R. Sudhölter, *J. Am. Chem. Soc.* **2005**, *127*, 2514–2523.

[14] N. Tajimi, H. Sano, K. Murase, K.-H. Lee, H. Sugimura, *Langmuir* **2007**, *23*, 3193–3198.

[15] L. C. P. M. de Smet, A. V. Pukin, Q.-Y. Sun, B. J. Eves, G. P. Lopinski, G. M. Visser, H. Zuilhof, E. J. R. Sudhölter, *Appl. Surf. Sci.* **2005**, *252*, 24–30.

[16] a) X. Wallart, C. H. de Villeneuve, P. Allongue, *J. Am. Chem. Soc.* **2005**, *127*, 7871 – 7878; b) R. Boukherroub, D. D. M. Wayner, *J. Am. Chem. Soc.* **1999**, *121*, 11513 – 11515.

[17] B. Fabre, G. P. Lopinski, D. D. M. Wayner, *J. Phys. Chem. B* **2003**, *107*, 14326 – 14335.

[18] a) S. Gowda, G. Mathur, V. Misra, *Appl. Phys. Lett.* **2007**, *90*, 142113 – 1–142113 – 3; b) E. A. Dalchiele, A. Aurora, G. Bernardini, F. Cattaruzza, A. Flamini, P. Pallavicini, R. Zanoni, F. Decker, *J. Electroanal. Chem.* **2005**, *579*, 133 – 142.

[19] P. Allongue, C. H. de Villeneuve, J. Pinson, *Electrochim. Acta* **2000**, *45*, 3241 – 3248.

[20] E_{fb} is the potential for which there is no space charge region in the semiconductor. For potentials $E \gg E_{fb}$, n-type silicon is under depletion conditions, that is, there are few majority charge carriers (namely, electrons) available for charge transfer.

[21] a) T. Gupta, M. E. van der Boom, *Angew. Chem.* **2008**, *120*, 5402 – 5406; *Angew. Chem. Int. Ed.* **2008**, *47*, 5322 – 5326; b) C. P. Collier, E. W. Wong, M. Belohradsky, F. M. Raymo, J. F. Stoddart, P. J. Keukes, R. S. Williams, J. R. Heath, *Science* **1999**, *285*, 391 – 394.